

## Supporting Information

### **Coaxial Extrusion Bioprinting of 3D Microfibrous Constructs with Cell-Favorable Microenvironments**

Wanjun Liu<sup>1,2,3</sup>, Zhe Zhong<sup>1,2</sup>, Ning Hu<sup>1,2</sup>, Yixiao Zhou<sup>1,2</sup>, Lucia Maggio<sup>1,2</sup>, Amir K Miri<sup>1,2</sup>, Alessio Fragasso<sup>1,2</sup>, Xiangyu Jin<sup>3</sup>, Ali Khademhosseini<sup>1,2,4</sup> and Yu Shrike Zhang<sup>1,2</sup>

<sup>1</sup> Biomaterials Innovation Research Center, Division of Engineering in Medicine, Brigham and Women's Hospital, Harvard Medical School, Cambridge, MA 02139, USA

<sup>2</sup> Harvard-MIT Division of Health Sciences and Technology, Massachusetts Institute of Technology, Cambridge, MA 02139, USA

<sup>3</sup> Key Laboratory of Textile Science and Technology, Ministry of Education, College of Textiles, Donghua University, Shanghai 201620, P.R. China

<sup>4</sup> Department of Bioindustrial Technologies, College of Animal Bioscience and Technology Konkuk University, Seoul 143-701, Republic of Korea

E-mail: [alik@bwh.harvard.edu](mailto:alik@bwh.harvard.edu) and [yszhang@research.bwh.harvard.edu](mailto:yszhang@research.bwh.harvard.edu)

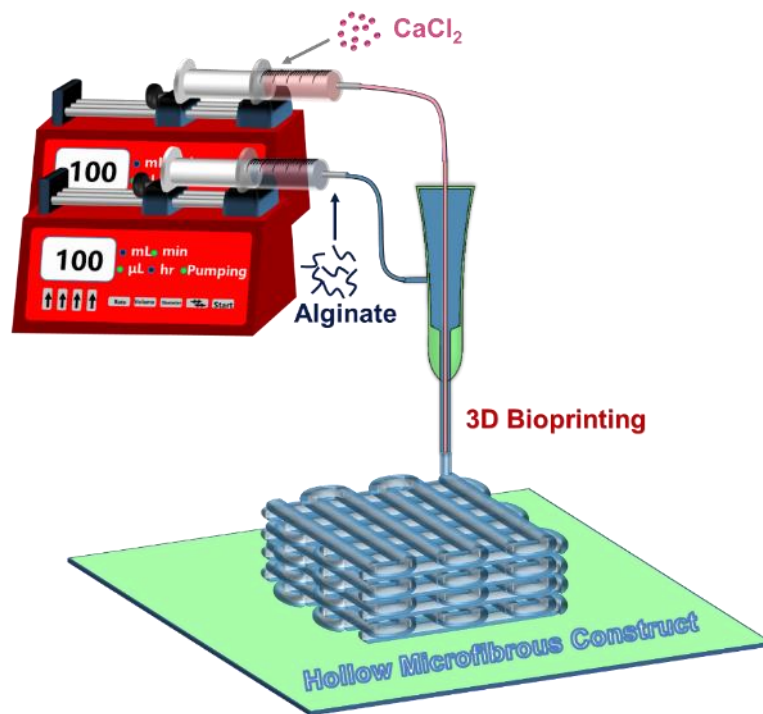


**Figure S1.** Schematic diagram showing the bioprinting of alginate hollow microfibrous constructs.

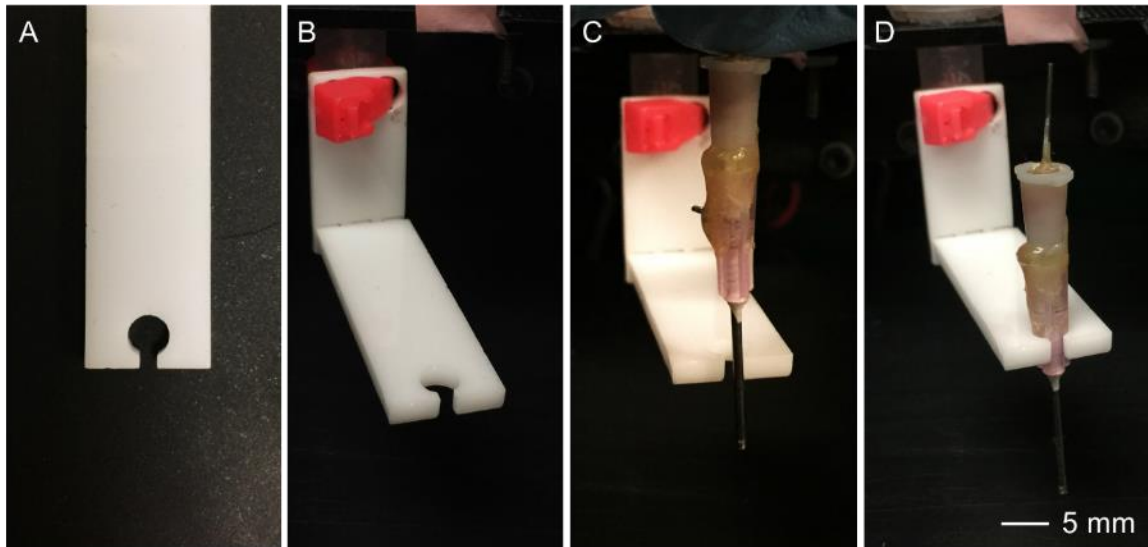


**Figure S2.** Photographs showing the custom-made printhead and core/sheath coaxial nozzle. A, B) The printhead. C, D) The installation of core/sheath coaxial nozzle onto the printhead.

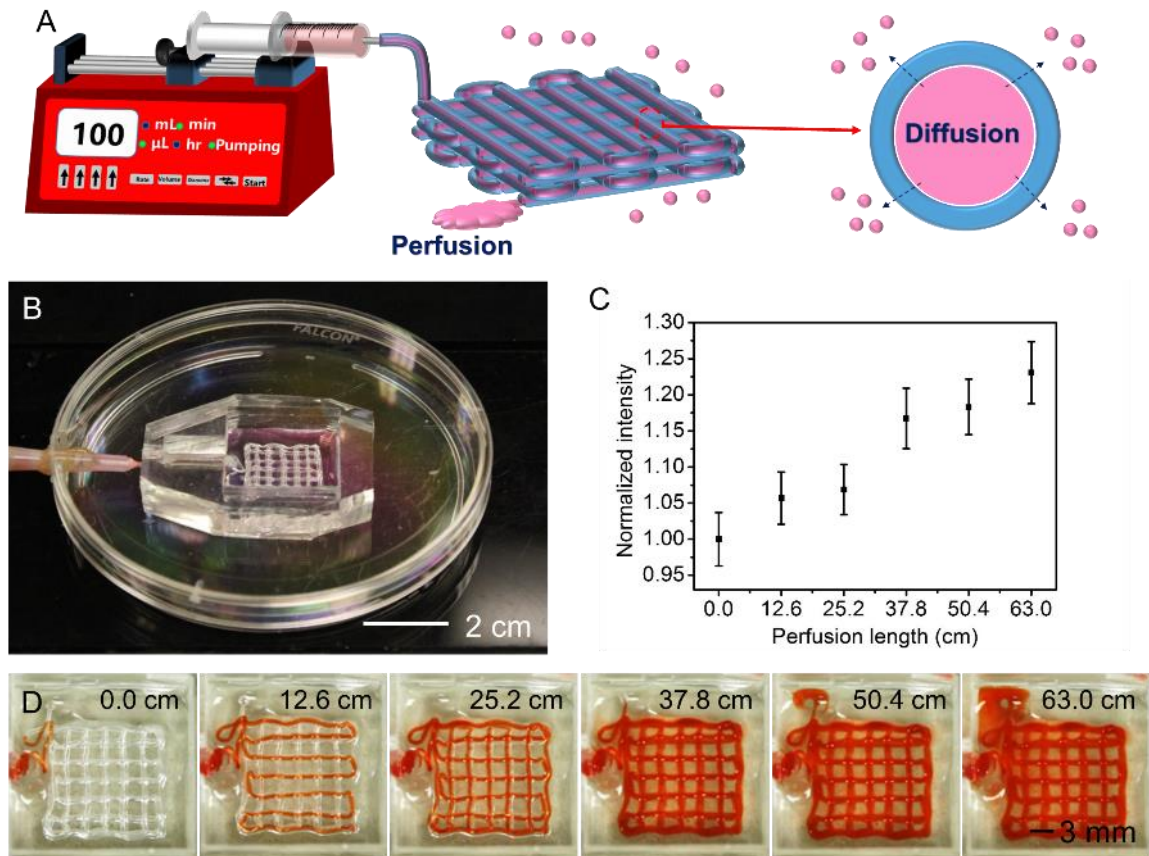


**Figure S3.** Perfusion and diffusion performance of the alginate hollow microfibrous constructs. A) Schematic diagram showing the diffusion during perfusion. B) Photograph of the perfusion device. C) Quantification of the diffusion process: normalized gray-scale intensity as a function of perfusion. D) Photographs showing the diffusion/perfusion.

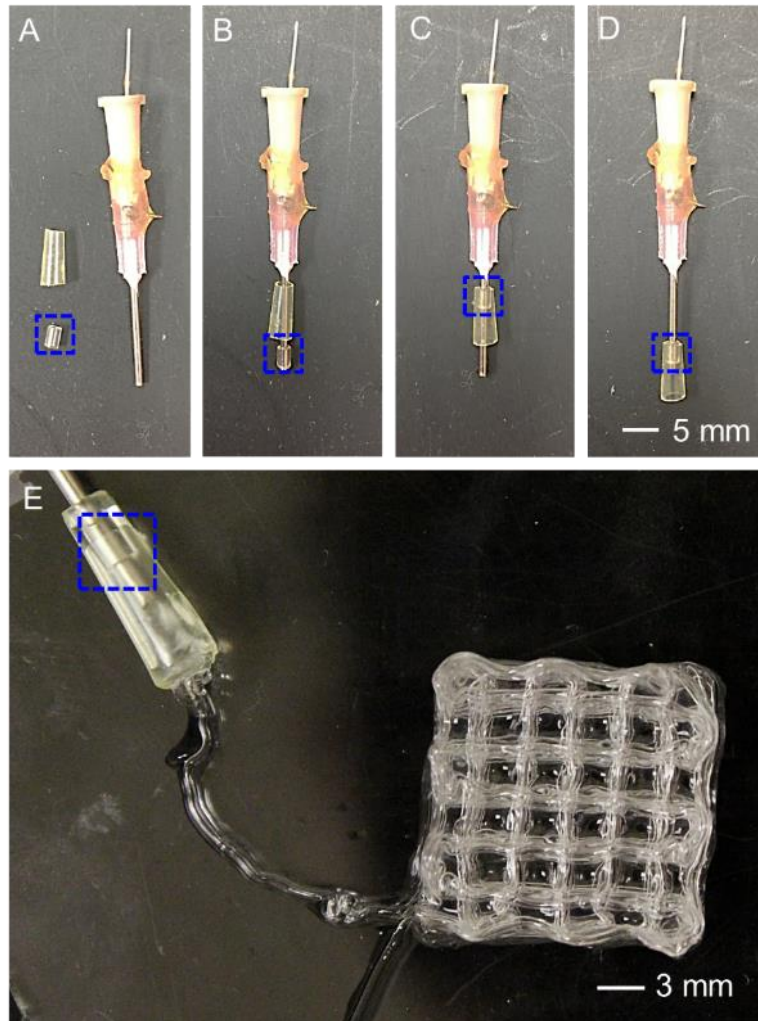


**Figure S4.** Photographs showing the custom-made core/sheath coaxial nozzle with a movable supporting device. A-C) The installation of the movable supporting device onto the nozzle. D) Downward movement of the device to support the connection between the nozzle and alginate microfiber after biprinting. E) A photograph showing perfusion.

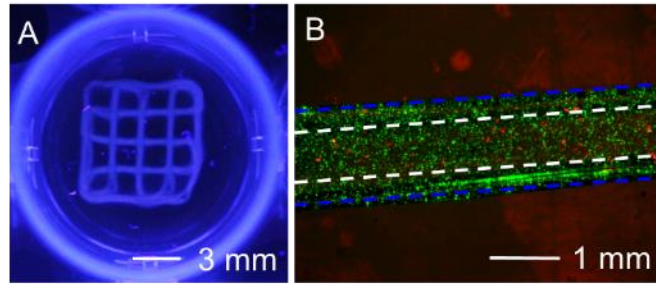


**Figure S5.** Biprinted GelMA/alginate core/sheath microfibrillar constructs. A) Photograph showing the entire structure. B) Fluorescence image showing the core/sheath structure of the microfiber, red and green fluorescent microbeads were used to visualize the core and sheath, respectively.

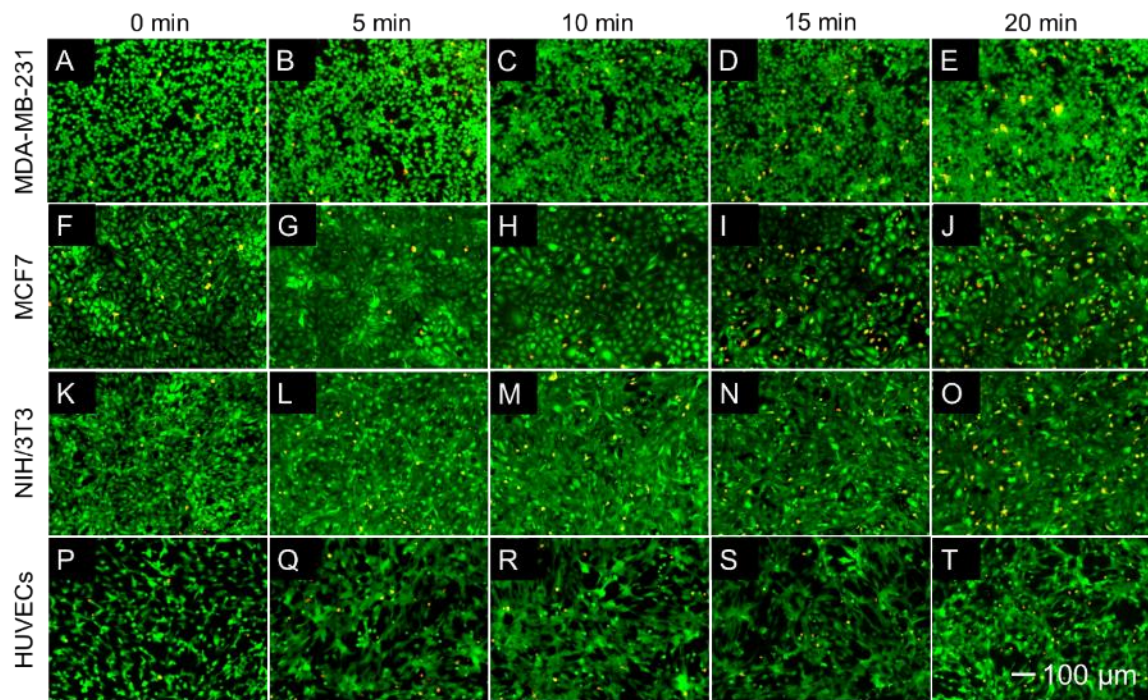


**Figure S6.** Live/Dead staining of cells cultured in 24-well plates over a 20-min culture with media containing 1.0%  $\text{CaCl}_2$ . A-E) MDA-MB-231. F-J) MCF7. K-O) NIH/3T3. P-T) HUVECs.

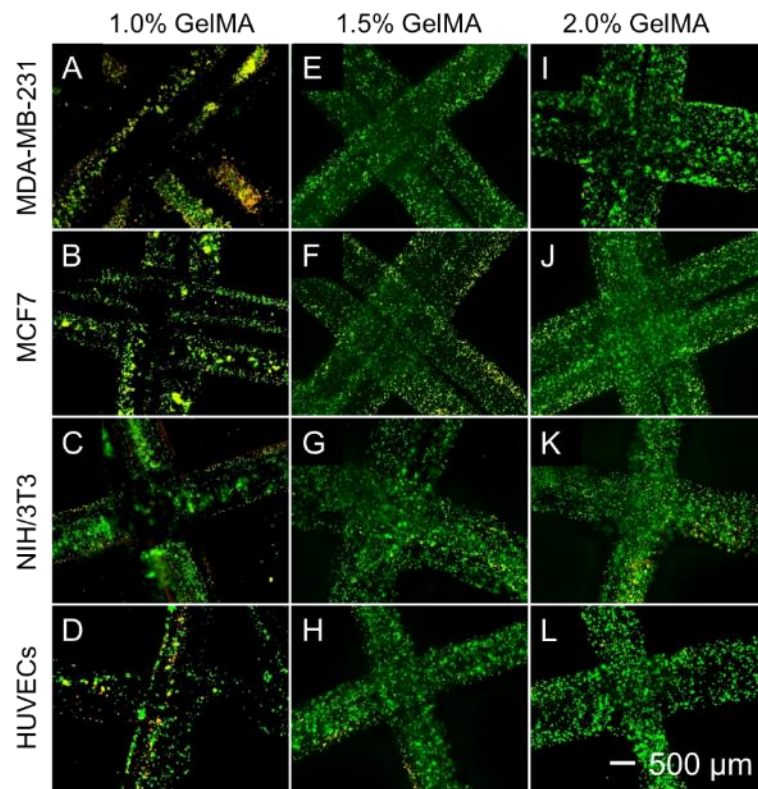


**Figure S7.** Live/Dead staining of cells in bioprinted GelMA/alginate constructs (Day 1). A-C) MDA-MB-231. D-F) MCF7. G-I) NIH/3T3. J-L) HUVECs.

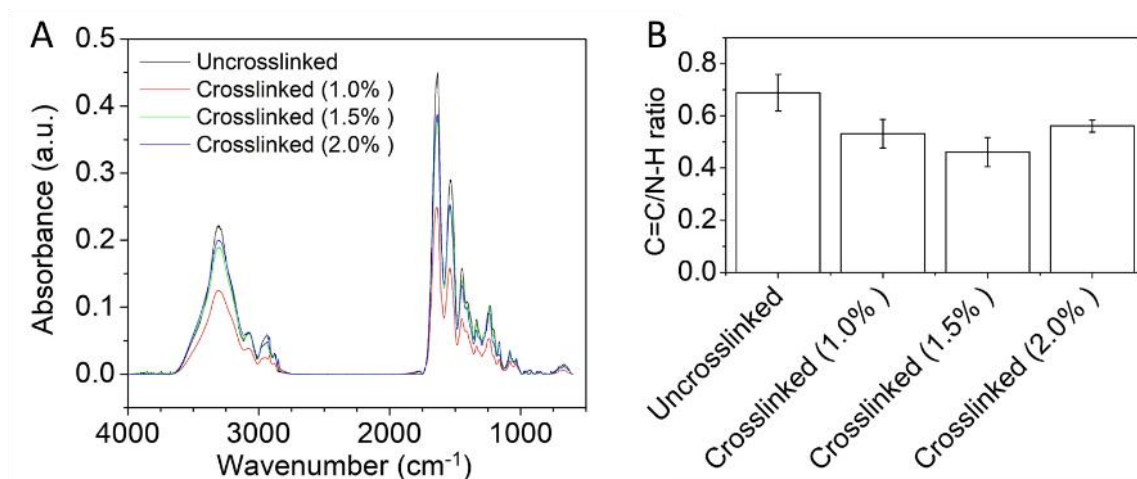


**Figure S8.** A) FTIR spectra of GelMA samples before and after crosslinking. GelMA showed its characteristic peak of N-H stretching at 3300 cm<sup>-1</sup> and unsaturated C=C peak at 1640 cm<sup>-1</sup> [1, 2]. B) Quantification of C=C/C-H ratio by calculating the ratio of integrated areas of absorbance in the ranges of 1580-1740 cm<sup>-1</sup> and 3110-3640 cm<sup>-1</sup>. Overall, the C=C/N-H ratio decreased after crosslinking, but no significant difference among the different concentrations was observed, indicating that the amount of C=C groups decreased after crosslinking, but the crosslinking efficiency almost did not change among the different concentrations. It should be noted that the uncrosslinked GelMA samples at different concentrations did not show significant difference and thus the representative spectrum of 1.5% GelMA sample was used.

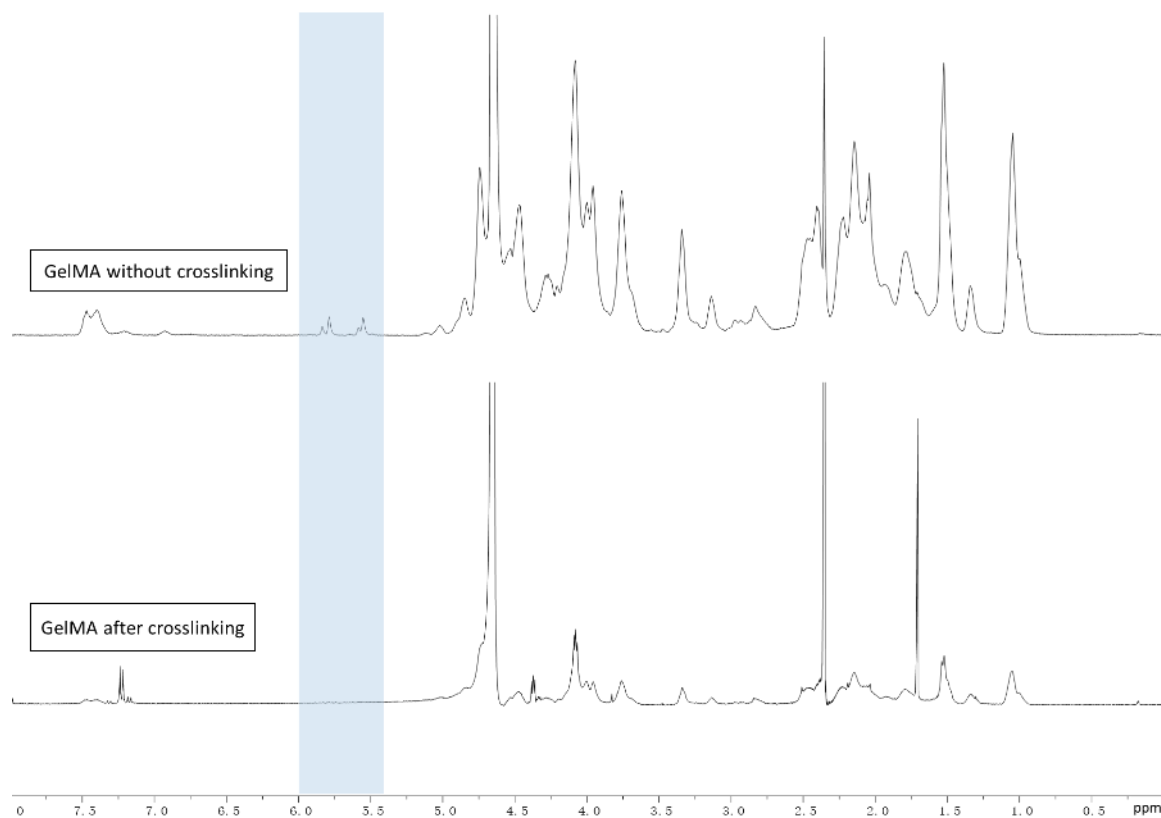


**Figure S9.**  $^1\text{H}$  NMR spectra of 1% GelMA samples before and after crosslinking. GelMA showed its characteristic peaks of methacryloyl groups between 5.4 and 6.0 ppm [3], while these peaks disappeared after crosslinking, suggesting that the crosslinking efficiency was high.

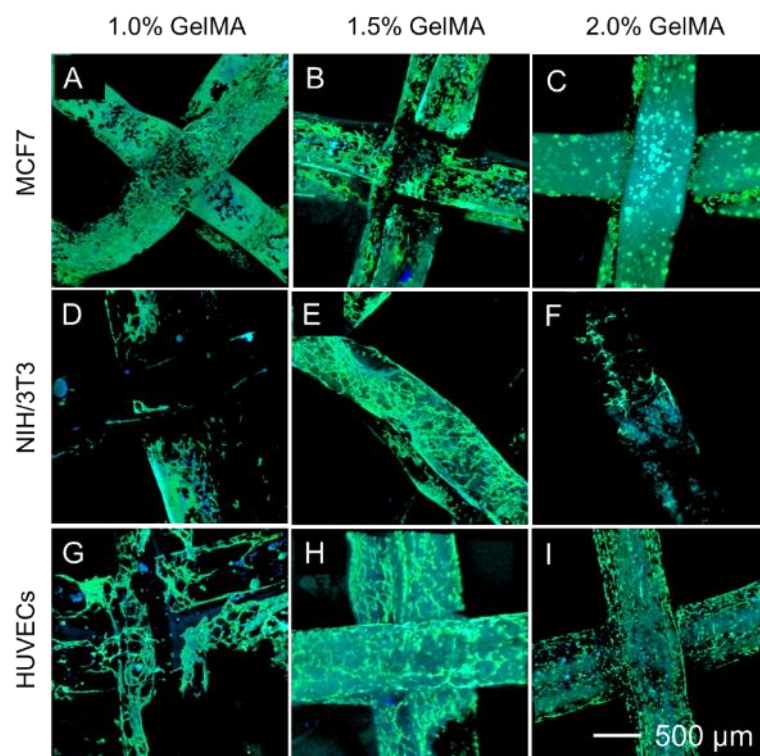
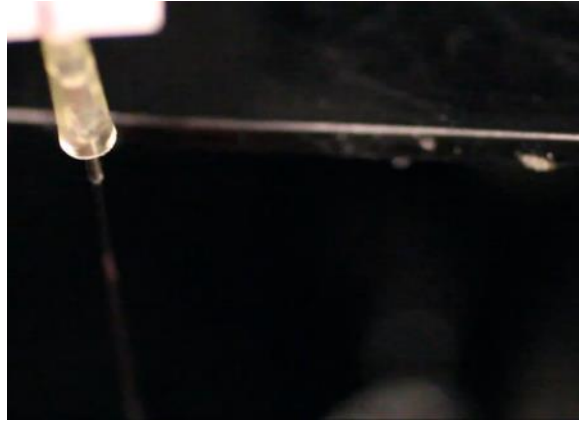
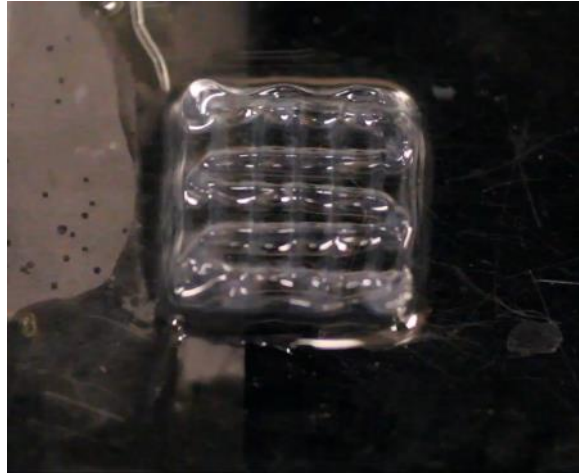


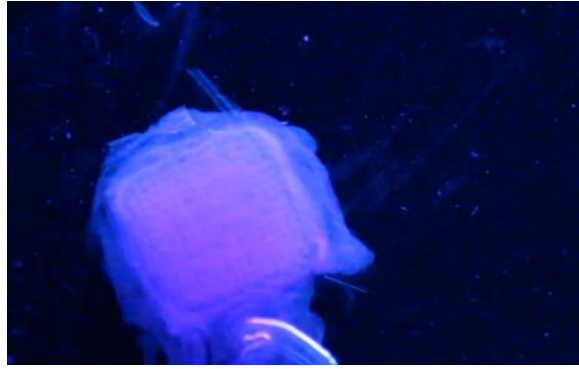
**Figure S10.** Fluorescence images showing cells stained for F-actin and nuclei in the bioprinted GelMA/alginate constructs at Day 9. A-C) MCF7. D-F) NIH/3T3. G-I) HUVECs.



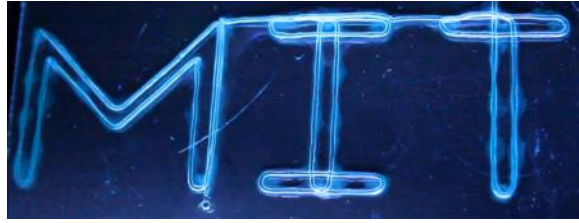
**Movie S1.** Bioprinting of alginate hollow microfibrous constructs.



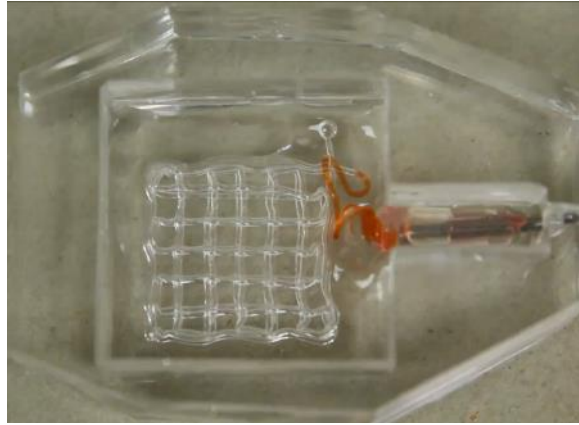
**Movie S2.** Perfusion of a 10-layer alginate hollow microfibrous construct with a distance between the contiguous microfibers of 2.3 mm.



**Movie S3.** Perfusion of a 10-layer alginate hollow microfibrous construct with a distance between the contiguous microfibers of 0.0 mm.



**Movie S4.** Perfusion of a “MIT”-patterned alginate hollow microfibrous construct.



**Movie S5.** Perfusion of alginate hollow microfibrous constructs.